

# GBT-based buckling analysis of composite steel-concrete beams

Carlos M. Andrade Júnior<sup>1</sup>, Cilmar D. Basaglia<sup>1</sup>

<sup>1</sup>*Department of Structural Engineering, School of Civil Engineering, Architecture and Urban Design, University of Campinas. 224 Saturnino de Brito St., 13083-889, São Paulo/Campinas, Brazil  
c262647@dac.unicamp.br, cbasaglia@fec.unicamp.br*

**Abstract.** Continuous restrained I-section beams may be subject to lateral-distortional buckling and web lateral buckling in regions of negative bending. Buckling analysis of restrained beams demands time-consuming Shell Finite Element Method (SFEM) models. SFEM is an important unquestionable tool to solve eigenvalue problems, however, it requires models involving several degrees of freedom and substantial engineering judgment. This fact explains why assessing the structural response of such structural systems constitutes a complex task. One very promising route that has been explored in the last decade is the use of Generalized Beam Theory (GBT) – a beam theory that incorporates genuine folded-plate concepts. In this context, a GBT-based analytical solution for the distortional buckling is proposed. First, the continuous elastic torsional restraint is incorporated in the cross-section distortional deformation mode. Next, a kinematic assumption comprising the null shear strain in each wall mid-plane is imposed to determine the distortional displacement field. Finally, the buckling stress is derived from an energy method. The accuracy of the solution is validated by numerical solutions provided by the 2.0 release of the software GBTUL.

**Keywords:** Distortional buckling, Generalized Beam Theory (GBT), Restrained deformation modes

## 1 Introduction

The distortional buckling may control the design of steel-concrete composite members in negative moment regions. The slab in-plane rigidity restrains the lateral displacement of the top flange while the lower flange performs a rigid-body motion. Bradford and Trahair [1] first addressed this instability phenomenon, were a Shell Finite Element Method (SFEM) was presented. Since then, several authors have studied this subject, and analytical [2-4] and numerical [5-8] solutions were presented.

More recently, Ye and Chen [9] has shown that analytical solutions proposed by Svensson [2], Williams and Jemah [3] and Goltermann and Svensson [4] has poor accuracy when compared to numerical solution calculated by an SFEM software, with maximum error ranging from -12% to 60% for a beam under a negative uniform moment.

Numerical solutions proposed by Johnson and Bradford [5], Bradford and Gao [6], Bradford and Ronagh [7], and Vrcelj and Bradford [8] require an SFEM algorithm implementation. Additionally, they often require models involving several degrees of freedom and substantial engineering judgment to characterize a buckling deformation mode. To overcome this problem, the authors developed an analytical solution for the distortional buckling of I-beams based on the Generalized Beam Theory (GBT) where the displacement field is represented by two degrees of freedom.

The critical buckling stress has been shown by Bradford [10] to asymptote to an upper bound as the rotational restraint increases while the lateral restraint has an insignificant impact on distortional buckling. Consequently, the assumption of an infinitely rigid rotational spring may result in a non-conservative design.

This paper analyzes two distortional buckling modes: (i) orthogonal distortional buckling combining lateral (rigid body) displacement of the unrestrained flange and distortion of the web and (ii) non-orthogonal distortional buckling involving double curvature of the web. First, the continuous elastic torsional restraint is incorporated in the cross-section analysis following a process similar to the procedure presented by Bebiano et al. [11]. Thenceforth, null shear strain assumption is imposed to determine the distortional displacement and the Galerkin

method is applied to calculate the buckling stress. To evaluate the efficacy of the GBT-based solution, two illustrative examples are calculated by the 2.0 release of the GBTUL (Bebiano et al. [12]), and the numerical results are compared with the analytical solution presented.

## 2 Cross-Section Analysis

The cross-section analysis is the first step in the GBT-based solution. The thin-walled section is discretized in distinct plates connected by natural nodes. The slab flexural and the axial stiffness are represented by  $k_r$  and  $k_t$  restraint coefficients, respectively, as illustrated in Fig. 1. According to Bradford [10], the effects of the minor axis elastic restraint on the distortional buckling are minimal, so the  $k_r$  are assumed to be infinitely large.

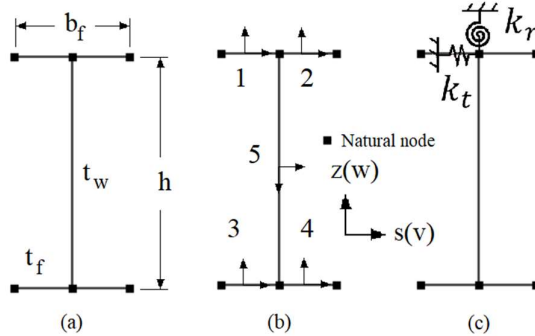


Figure 1. (a) Cross-section geometry, (b) nodal discretization, local axes, and plate numbering, (c) slab restraint coefficients

The warping elementary modes correspond to the imposition of a unit out-of-plane displacement at a natural node and null displacements at the others. The cross-section is analyzed as a spatial truss model. The warping displacement  $u(s)$  is approximated by a linear polynomial. The in-plane elementary modes correspond to the imposition of a unit in-plane displacement at a natural node (Fig. 2). The cross-section is analyzed as a plane frame model and the in-plane displacements -  $v(s)$  and  $w(s)$  - are approximated by linear and cubic polynomials, respectively.

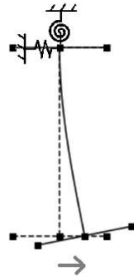


Figure 2. Elementary mode 1 (in-plane)

The standard cross-section analysis procedure presented by Bebiano et al. [11] involves a total of  $3 n_t$  ( $n_t$  – total number of nodes) elementary modes, corresponding to the imposition of 3 unit displacements at each node: two in-plane and one out-of-plane (warping) displacements. The present paper addresses only the elementary modes associated with the distortional buckling modes. In addition, these modes deviate from the standard procedure since some of these combine two elementary modes.

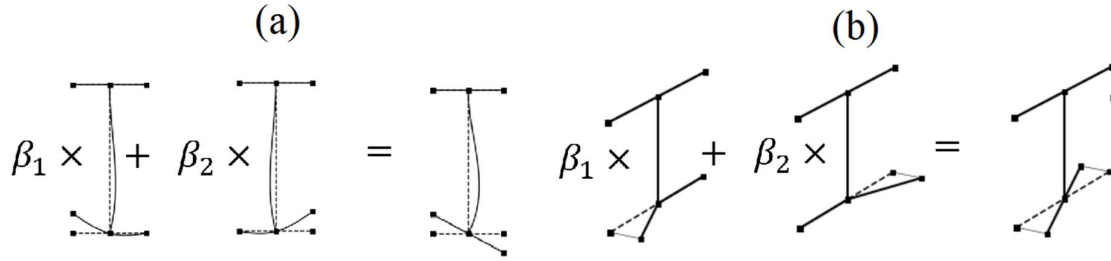


Figure 3. Mode combination associated to (a) mode 2 and (b) mode 3

Mode 2 illustrated in Fig. 3 represents a local deformation mode while modes 1 and 3 compose a base space for the orthogonal deformation mode. The set composed by modes 1 and 3 should be divided in two sub-spaces: (i) one concerning null shear deformation and (ii) another concerning non-null shear deformation. These sub-spaces are determined by the null (null shear) and non-null (non-null shear) eigenvalues of the generalized eigenvalue problem:

$$(\mathbf{D}^m - \lambda \mathbf{I})\mathbf{a} = \mathbf{0} \tag{1}$$

where  $\mathbf{I}$  is an identity matrix and  $\mathbf{D}^m$  is a stiffness matrix defined by:

$$D_{ik}^m = \int_{\Gamma} Gt(u_{i,s} + v_i)(u_{k,s} + v_k) ds \tag{2}$$

where the  $u_{i,s}$  is a short notation to express the derivative. The null solution of eq. (1) represents the orthogonal distortional mode and the non-orthogonal distortional mode is a linear combination of the first and the local deformation mode as illustrated in Fig. 4:

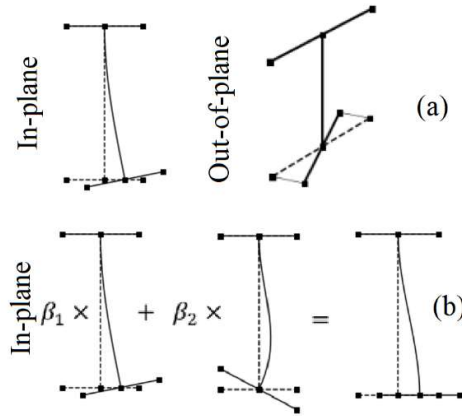


Figure 4. (a) Orthogonal distortional mode and (b) Non-orthogonal distortional mode

After performing the cross-section analysis, it is possible to determine the displacement field related to the orthogonal distortional mode and the local mode. The displacement field associated to the orthogonal distortional mode in the matrix form is given by:

$$u_D(s) = \begin{bmatrix} 0 \\ 0 \\ 1 - 2/b_f s \\ -2/b_f s \\ 0 \end{bmatrix}, v_D(s) = \begin{bmatrix} 0 \\ 2/b_f \\ 2/b_f \\ 0 \end{bmatrix}, \text{ and } w_D(s) = \begin{bmatrix} -\alpha_D b_f/2 (1 - 2/b_f s) \\ \alpha_D s \\ -\beta_D b_f/2 (1 - 2/b_f s) \\ \beta_D s \\ a_1 s + a_2 s^2 + a_3 s^3 \end{bmatrix}. \tag{3}$$

The displacement field associated to the local mode in the matrix form is given by:

$$u_L(s) = \begin{bmatrix} 0 \\ 0 \\ 0 \\ 0 \\ 0 \end{bmatrix}, v_D(s) = \begin{bmatrix} 0 \\ 0 \\ 0 \\ 0 \\ 0 \end{bmatrix}, \text{ and } w_D(s) = \begin{bmatrix} -\alpha_L b_f/2 \left(1 - 2/b_f s\right) \\ \alpha_L s \\ -\beta_L b_f/2 \left(1 - 2/b_f s\right) \\ \beta_L s \\ b_1 s + b_2 s^2 + b_3 s^3 \end{bmatrix}. \quad (4)$$

$\alpha$  and  $\beta$  are the top and lower flanges mid-node rotation angles.  $a_i$  and  $b_i$  are coefficients depending on the flexural stiffness of the web plate. The mid-line functions follow the local axes convention and node numbering presented in Fig. 1.

### 3 Buckling Analysis

After determining the fundamental modes associated with distortional instability, it becomes possible to perform a buckling analysis. The cross-section displacement field is approximated by a linear combination of the orthogonal distortional mode and the local mode:

$$\begin{aligned} u(x, s) &= u_D(s)\phi_{D,x}(x) \\ v(x, s) &= v_D(s)\phi_D(x) \\ w(x, s) &= w_D(s)\phi_D(x) + w_L(s)\phi_L(x) \end{aligned} \quad (5)$$

where the subscript D and L indicate the distortional and local modes, respectively.  $u_k(s)$ ,  $v_k(s)$ , and  $w_k(s)$  are the mid-line functions defining the cross-section deformation mode  $k$ .  $\phi_k(x)$  is the amplitude function describing the variation along the member length of mode  $k$ .  $\phi_k(x)$  should be expressed in the following form:

$$\begin{aligned} \phi_L(x) &= a_L \bar{\phi}(x) \\ \phi_D(x) &= a_D \bar{\phi}(x) \end{aligned} \quad (6)$$

where (i)  $a_D$  and  $a_L$  are amplitude coefficients of modes D and L (ii)  $\bar{\phi}(x)$  is a function describing, exactly or approximately, the variation along the longitudinal direction. For a simply supported beam subject to a uniform moment the exact function – which satisfies both natural and essential boundary conditions – is given by:

$$\bar{\phi}(x) = \sin\left(\frac{n\pi x}{L}\right) \quad (7)$$

where  $n$  is the number of half-wavelengths.

The functions  $u(x, s)$  and  $v(x, s)$  depend exclusively on the distortional mode because the local mode is comprised only by in-plane displacement  $w_L(s)$ . The buckling behavior of a restrained beam is governed by the differential equation system relatively to modes D and L:

$$\mathbf{K} + \mathbf{R} + \lambda \mathbf{G} = \mathbf{0} \quad (8)$$

where  $\mathbf{K}$  is the first-order stiffness matrix,  $\mathbf{R}$  is the continuous restraint stiffness matrix and  $\mathbf{G}$  is the second-order (geometric) matrix given by:

$$\begin{aligned} K_{ik} &= C_{ik}\phi_{k,xxxx} - (D_{ik} - E_{ik} - E_{ki})\phi_{k,xx} + B_{ik}\phi_k \\ R_{ik} &= k_r \alpha_{ik}^2 \phi_k \\ G_{jik} &= \phi_{j,xx}^0 X_{jik} \phi_{k,xx} \end{aligned} \quad (9)$$

where  $B_{ik}$ ,  $C_{ik}$ ,  $D_{ik}$  and  $E_{ik}$  are stiffness matrices given by:

$$\begin{aligned}
 C_{ik} &= \int_{\Gamma} Et u_i u_k ds + \int_{\Gamma} \frac{Et}{12(1-\nu^2)} w_i w_k ds \\
 B_{ik} &= \int_{\Gamma} \frac{Et}{1-\nu^2} v_{i,s} v_{k,s} ds + \int_{\Gamma} \frac{Et^3}{12(1-\nu^2)} w_{i,ss} w_{k,ss} ds \\
 D_{ik} &= \int_{\Gamma} Gt(u_{i,s} + v_i)(u_{k,s} + v_k) ds + \int_{\Gamma} \frac{Gt^3}{3} w_{i,s} w_{k,s} ds \\
 E_{ik} &= \int_{\Gamma} \frac{\nu Et}{1-\nu^2} u_i v_{k,s} ds + \int_{\Gamma} \frac{\nu Et^3}{12(1-\nu^2)} w_i w_{k,ss} ds \\
 X_{jik} &= \int_{\Gamma} \sigma_{xx}^0 t (v_i v_k + w_i w_k) ds
 \end{aligned} \tag{10}$$

where (i)  $\Gamma$  stands for the mid-line domain, (ii)  $\sigma_{xx}^0(s)$  and  $\phi_j^0(x)$  are the pre-buckling normal stress function and modal amplitude functions, respectively, (iii)  $E$  is the Young modulus and  $\nu$  is the Poisson ratio. They can be determined by a first-order (pre-buckling) analysis, as defined in Bebiano et al. [12]. Equation (8) should be solved by the Galerkin method, which results:

$$|\tilde{\mathbf{K}} + \tilde{\mathbf{R}} - \lambda \tilde{\mathbf{G}}| = 0 \tag{11}$$

where:

$$\begin{aligned}
 \tilde{K}_{ik} &= \frac{n^4 \pi^4}{L^4} C_{ik} + \frac{n^2 \pi^2}{L^2} (D_{ik} - E_{ik} - E_{ki}) + B_{ik} \\
 \tilde{R}_{ik} &= k_r \alpha_{ik}^2 \\
 \tilde{G}_{ik} &= -\frac{n^2 \pi^2}{L^2} \phi_{j,xx}^0 X_{jik}.
 \end{aligned} \tag{12}$$

The characteristic polynomial roots are:

$$\lambda = \frac{-\eta_2 \pm \sqrt{\eta_2^2 - 4\eta_1\eta_3}}{2\eta_1} \tag{13}$$

where

$$\begin{aligned}
 \eta_1 &= -\tilde{G}_{DL}^2 + \tilde{G}_{DD} \tilde{G}_{LL} \\
 \eta_2 &= -\tilde{G}_{LL}(\tilde{K}_{DD} + \tilde{R}_{DD}) - \tilde{G}_{DD}(\tilde{K}_{LL} - \tilde{R}_{LL}) + 2\tilde{G}_{DL}(\tilde{K}_{DL} + \tilde{R}_{DL}) \\
 \eta_3 &= -\tilde{K}_{DL}^2 + \tilde{K}_{LL} \tilde{R}_{DD} - 2\tilde{K}_{DL} \tilde{R}_{DL} - \tilde{R}_{DL}^2 + \tilde{R}_{DD} \tilde{R}_{LL} + \tilde{K}_{DD}(\tilde{K}_{LL} + \tilde{R}_{LL}).
 \end{aligned} \tag{14}$$

## 4 Illustrative Examples

In order to illustrate and validate the analytical solution proposed, two cross-section geometries were chosen the (i) orthogonal and (ii) non-orthogonal distortional buckling modes:

(i) Section 1:  $h = 200 \text{ mm}$ ,  $b_f = 100 \text{ mm}$ ,  $t_w = 1 \text{ mm}$ ,  $t_f = 2 \text{ mm}$ ,  $k_r = 10000 \text{ N}$ ;

(ii) Section 2:  $h = 200 \text{ mm}$ ,  $b_f = 100 \text{ mm}$ ,  $t_w = 1 \text{ mm}$ ,  $t_f = 10 \text{ mm}$ ,  $k_r = 100000 \text{ N}$ .

Section 1 has the same cross-section characteristics adopted by Silvestre [13]. A Young's modulus of 210 GPa and a Poisson ratio of 0.3 were assumed.

The critical stress variation as a function of the rotational stiffness  $k_r$  is plotted in Fig. 5 for a beam length of 4662 mm. It corresponds to the critical length related to the orthogonal distortional mode considering a full rotation

restraint at the top flange. The critical stress asymptotes the value calculated by Silvestre [13], which considers a full rotational restraint. This author also suggested that I-sections with a very thick flange exhibit a buckling mode comprising double curvature of the web (non-orthogonal distortional). This hypothesis was confirmed by the analytical and numerical results in Fig. 5.

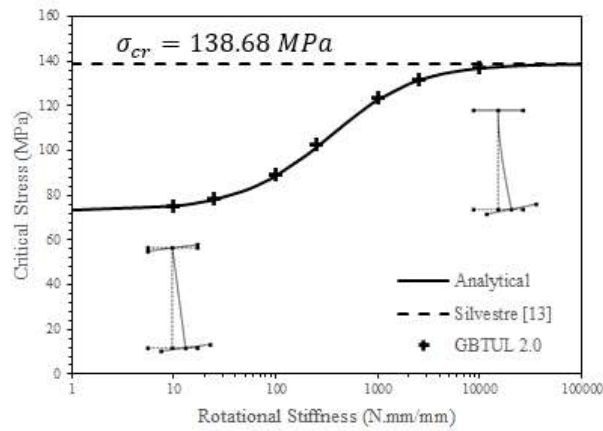


Figure 5. Critical stress variation with the rotational stiffness

The critical stress variation with the beam length for Section 1 (a) and Section 2 (b) are plotted in Fig. 6. It is seen that analytical and numerical solutions are in close agreement. Section 1 exhibits a local mode instability at the beam length interval of  $5600 < L < 7600 \text{ mm}$ , corresponding to the transition between one and two half-wavelengths. This phenomenon does not affect Section 2 distortional mode.

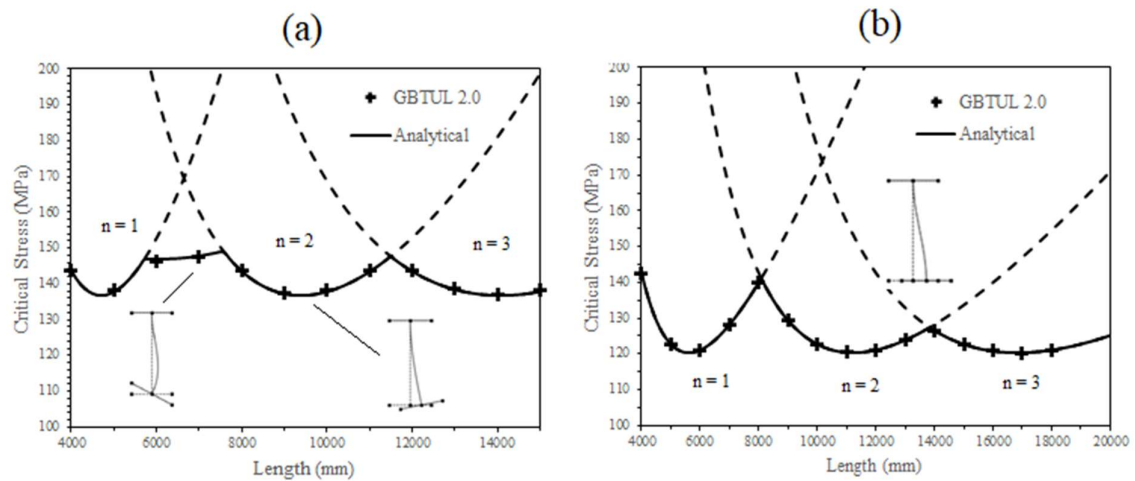


Figure 6 - Critical stress variation with the beam length for (a) Section 1 and (b) Section 2

## 5 Conclusions

The present paper presented a GBT-based analytical solution for the distortional buckling of composite steel-concrete beams. Two instability modes were covered: (i) lateral distortional buckling for I-sections with thin flanges, and (ii) web lateral buckling for cross-sections with thick flanges. The GBT enabled the derivation of an accurate closed-form solution determined by a linear combination of only two degrees of freedom, while an SFEM solution would require an extensive computational cost. The illustrative examples provided demonstrated that the distortional critical stress asymptotes to a maximum as the rotational coefficient increases, confirming previous studies. This fact explains why the consideration of an infinitely rigid rotational spring may lead to a non-conservative design. Numerical and analytical results also demonstrated that a local buckling mode might control the design of I-sections with thin flanges.

**Acknowledgments.** The first author would like to thank the Conselho Nacional de Desenvolvimento Científico e Tecnológico do Brasil (CNPq) for the financial support provided through the master's degree scholarship.

**Authorship statement.** The authors hereby confirm that they are the sole liable persons responsible for the authorship of this work, and that all material that has been herein included as part of the present paper is either the property (and authorship) of the authors, or has the permission of the owners to be included here.

## References

- [1] M.A. Bradford and N.S. Trahair. "Distortional buckling of thin-web beam-columns". *Engineering Structures*, vol. 4, n. 4, pp. 2-10, 1982.
- [2] S.E. Svensson. Lateral buckling of beams analysed as elastically supported columns subject to a varying axial force. *Journal of Construction Steel Research*, vol. 5, n. 3, pp.179-193, 1985.
- [3] F.W. Williams and A.K. Jemah. Buckling curves for elastically supported columns with varying axial force to predict lateral buckling of beams. *Journal of Construction Steel Research*, vol. 7, n. 2, pp.133-147, 1987.
- [4] P. Goltermann and S. E. Svensson. Lateral distortional buckling: Predicting elastic critical stress. *Journal of Structural Engineering*, vol. 114, n. 7, pp. 1606-1625, 1988.
- [5] R.P. Johnson and M.A. Bradford. Inelastic buckling of composite bridge girders near internal supports. *Proceedings of the Institution of Civil Engineers*. Vol. 83, n. 1, pp. 143-159, 1987.
- [6] M. Bradford and Z.Gao. Distortional buckling solutions for continuous composite beams. *Journal of Structural Engineering, ASCE*, vol. 118. pp. 73-89, 1992.
- [7] M.A. Bradford and H.R. Ronagh. Generalized elastic buckling of restrained I-beams by FEM. *Journal of Structural Engineering, ASCE*, vol. 123, n. 12, pp. 1631-1637, 1997.
- [8] Z. Vrcelj and M.A. Bradford. Elastic distortional buckling of continuously restrained I-section beam-columns. *Journal of Construction Steel Research*, vol. 62, n. 3, pp.223-230, 2006.
- [9] J.H. Ye and W. Chen. Elastic restrained distortional buckling of steel-concrete composite beams based on elastically supported column method. *International Journal of Structural Stability and Dynamics*, vol. 13, n. 1, 2013.
- [10] M.A. Bradford. Buckling of elastically restrained beams with web distortions. *Thin-Walled Structures*, vol. 6, n. 4, pp. 287-34, 1988.
- [11] R. Bebiano, R.Gonçalves and D. Camotim. A cross-section analysis procedure to rationalise and automate the performance of GBT-based structural analyses. *Thin-Walled Structures*, vol. 92, pp. 29-47, 2015.
- [12] R. Bebiano, D. Camotim and R. Gonçalves. GBTUL 2.0 – A second-generation code for the GBT-based buckling and vibration analysis of thin-walled members. *Thin-Walled Structures*, vol. 124, pp. 235-257, 2018.
- [13] N. Silvestre. Distortional mechanics of restrained steel sections. *Journal of Construction Steel Research*, vol. 66, n. 7, pp.873-884, 2010.